Journal of Alloys and Compounds 488 (2009) 360–363

Contents lists available at ScienceDirect

Journal of Alloys and Compounds

journal homepage: www.elsevier.com/locate/jallcom

Studies of Mg film and substrate coupling effects on hydrogenation properties

L. Pranevicius[a,*], D. Milcius[b], C. Templier[c], L.L. Pranevicius[a], M. Lelis[a,b]

[a] Vytautas Magnus University, 8 Vileikos St., LT-44404 Kaunas, Lithuania
[b] Lithuanian Energy Institute, 3 Breslaujos St., LT-44403 Kaunas, Lithuania
[c] Université de Poitiers, SP2MI, Bd Marie et Pierre Curie, 30179 Futuroscope, France

ARTICLE INFO

Article history:
Received 2 July 2009
Received in revised form 26 August 2009
Accepted 27 August 2009
Available online 1 September 2009

Keywords:
Mg
MgH_2
Thin films
Hydrogen
Coupling

ABSTRACT

Changes of microstructure, phase composition and surface morphology were investigated for 1.5–2 μm thick nanocrystalline Mg films, which were sputter-deposited on quartz and stainless steel substrates and hydrogenated at 600 kPa in the temperature range 200–260 °C. The volume fraction of MgH_2 in Mg and changes of the surface topography were analyzed using X-ray diffraction and scanning electron microscopy analysis, respectively. Coupling processes occurring between the Mg film and the substrate were registered and correlated with hydrogenation properties. Due to strong coupling to stainless steel substrate, a fast and complete transformation of Mg into MgH_2 accompanied by film cracking and spontaneous crushing into nanometer-size powder was observed. For Mg films weakly coupled to the quartz substrate, a slow and partial transformation of Mg into MgH_2 and simultaneous film buckling followed by film detachment and flaking was registered.

1. Introduction

Thin films exhibit physical properties contrasting with those from related bulk materials. It results from both the deposition method and the concomitant two-dimensional nature of the films. These particular physical properties mainly originate from: the presence of mixed crystalline and/or amorphous phases, film residual stresses resulting in some degree from disparities in film–substrate thermal properties, crystallite grain size, crystallite orientation and non-stoichiometry [1,2].

The fundamental difference with respect to bulk samples is the presence of a substrate which might alter kinetics and thermodynamics of the processes [3]. Hydrogen introduced in metals dilates the host lattice. Thin film is clamped to the substrate and therefore cannot expand freely in the in-plane direction as hydrogen concentration increases in it. Adhesion forces at the film–substrate interface act in opposite direction to prevent the expansion of the film, creating considerable in-plane stresses of the order of several GPa [4]. Consequently, hydrogenation of thin metallic films induces higher stresses than hydrogenation of bulk metals. It generates large compressive in-plane stresses, microstructural defects and ultimately large plastic deformations [5,6]. Usually nucleation rates of new phases involve free energies which are extraordinary sensitive to the conditions under which the experiment is run: pressure, impurity concentrations as well as temperature. Reproducibility of experimental data is difficult to achieve and the theoretical prediction of nucleation rate is subject to large uncertainties. It is therefore of primary importance to understand effects of the coupling between Mg films and the substrate on hydrogenation properties.

Many attempts have been undertaken to understand the dominant hydride synthesis mechanism by modifying the surface properties, reducing the particle size, controlling the surface oxidation or adding various elements [7,8]. However, the understanding of the processes for hydrogenation reaction is not complete. This is because the hydrogenation kinetics depends strongly on many surface and bulk material properties such as particle size and morphology, film microstructure, impurities and material fabrication technology. The present study focuses on the effects of coupling between the Mg film and the substrate on the synthesis kinetics of the hydride phase MgH_2.

2. Experimental details

Two micrometers thick Mg films were deposited onto either 304L stainless steel or quartz substrates in a vacuum device where the ultimate pressure obtained using cryogenic pumps was around 10^{-6} Pa. Steel coupons were electro-polished to remove the oxide layer and contaminants from the surface and then cleaned with methyl alcohol in an ultrasonic bath finally blow-dried with nitrogen. The surface roughness of substrates was estimated using atomic force microscopy (AFM) and it did not exceed 10 nm. As the substrate holder was not cooled, the temperature increased up to 80–120 °C during deposition, depending on the processing parameters. The Mg deposition rate of 0.3 nm s^{-1} was determined from the slope of the sample weight change, measured using a microbalance with a weight uncertainty of 2 μg which corresponds to an uncertainty of 10 nm on the thickness. The films grew in the shape of closely stacked columns extending throughout the film thickness, while containing polycrystalline grains and grain boundary defects, according

* Corresponding author. Tel.: +370 37 327909; fax: +370 37 327916.
E-mail address: l.pranevicius@gmf.vdu.lt (L. Pranevicius).

0925-8388/$ – see front matter © 2009 Elsevier B.V. All rights reserved.
doi:10.1016/j.jallcom.2009.08.133

to the commonly observed growth-mode of the Mg hexagonal basal plane parallel to the substrate plane [9]. The "Scotch Tape Test" was used to measure the adhesion strength of the Mg thin film to its substrate. An adhesive tape was applied to the film and subsequently pulled off and adhesion strength was considered "good" as the film stayed attached to the substrate. After deposition, the films were exposed in air and moved into a stainless steel cell for hydrogenation which was thoroughly flushed with pure H_2 (99.999%). The hydrogenation parameters (a steady-state temperature of 250 °C and a hydrogen pressure of 600 kPa) were reached after 7 min. The heating was turned off after the hydrogenation, Ar gas was injected and samples were cooled down during 16 h.

The microstructure of films was analyzed using X-ray diffraction (XRD) in the Bragg-Brentano configuration using CuK_α wavelength, with 2Θ angle in the range 20–70° in steps of 0.05°. The broadening of the diffraction peaks originated from the combined effect of the size of the coherently diffracting domains, microstrains (non-uniformly strained grains) and instrumental contributions (beam divergence, detector resolution). The different contributions were obtained by peak fitting using a Voigt function [10] and assuming that the Lorentzian and Gaussian components of the structurally broadened profile were due to size and strain broadening, respectively [11]. In practice, a reasonable estimate of the crystallite domain size was obtained using the Scherrer equation $D = \lambda/\beta_L \cos\Theta$, where β_L is the Lorentzian integral width and $\lambda = 1.5418$ Å is the wavelength of the Cu $K_{\alpha 1}$ source. The Lorentzian integral width β_L is related to the full width at half maximum ω_L of the Lorentzian component by $\beta_L = (\omega_L - \omega_L^i)/0.63662$, where ω_L^i is the instrumental contribution to the Lorentzian width obtained from the fitting of the (0 1 2) Al_2O_3 single crystal substrate peak. The identification of phases has been performed using Crystallographica Search-Match program [12]. The volume fraction of the hydride phase was calculated by means of the equation proposed in [13].

Scanning electron microcopy (SEM) using the JOEL JSM-6300 was also performed in parallel with AFM to characterize surfaces and undersides of as-deposited and hydrogenated films.

3. Results and discussion

XRD patterns of Mg films sputter deposited and hydrogenated on quartz or on stainless steel are displayed in Figs. 1 and 2, respectively, for different durations of hydrogenation. The XRD pattern of the as-deposited Mg film on the quartz substrate (Fig. 1, curve a) exhibits the characteristic h-Mg (0 0 2) peak at 34.5°. An evaluation of the mean size of crystallites gives 85 nm. A fast formation rate of hydride phase was registered during the initial stages of hydrogenation. The t-MgH_2 (1 0 1) and (2 0 0) peaks are observed at 35.8° and 40.2°, respectively, after only 15 min of hydrogenation, despite it took 7 min to reach the steady-state temperature and pressure. After 3 h of hydrogenation, the h-Mg (1 0 1) peak appears at 36.7° (Fig. 1, curve c). Significant modifications of the XRD pattern are registered after 6 h of hydrogenation: an additional peak corresponding to t-MgH_2 (1 1 0) is recorded at 27.9° and the t-MgH_2 (2 0 0) peak at 40.2° sharply increases while the h-Mg (1 0 1) peak at 36.7° decreases. These observations indicate that the structure of Mg film is dynamic. The volume of MgH_2 in the matrix of Mg increases forming nanocrystallites of different orientation. The observed broadening of the diffraction peaks for MgH_2 and Mg as hydrogenation proceeds can be related to the introduction of high concentration of defects in the dominant material, the increase of the lattice microstrain as well as to the decrease of the average crystallite size. However, the microstrain and the effect of damage were not taken into account to estimate the mean crystallite size of about 30 nm after 6 h of hydrogenation.

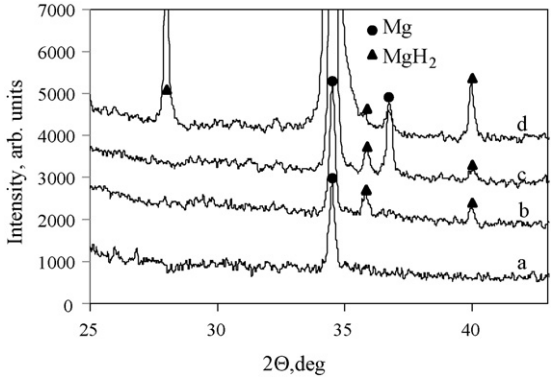

Fig. 1. XRD patterns of Mg films on quartz after different durations of hydrogenation: (a) as-deposited, (b) 15 min, (c) 180 min, and (d) 360 min.

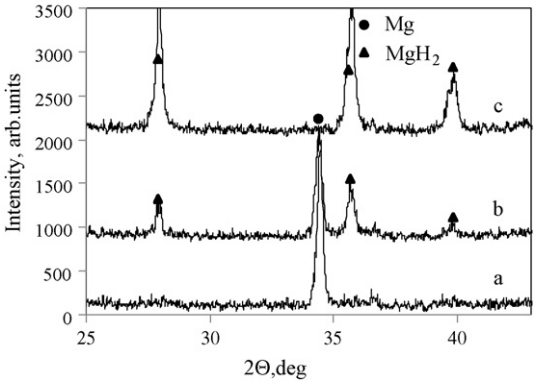

Fig. 2. XRD patterns of Mg films on stainless steel 304L substrate after different durations of hydrogenation: (a) as-deposited, (b) 15 min, and (c) 30 min.

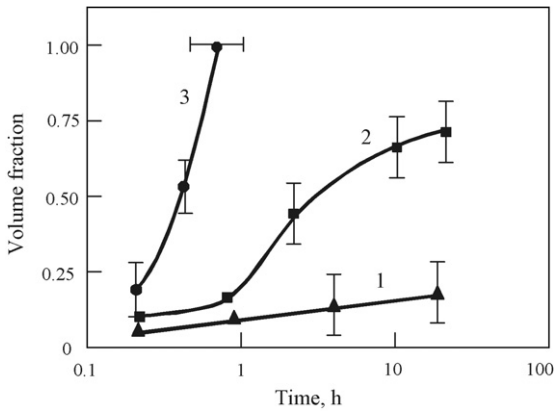

Fig. 3. Dependences of the volume fraction of the MgH_2 in Mg deposited on quartz at 220 °C (curve 1) and 250 °C (curve 2), and on stainless steel at 220 °C (curve 3) on hydrogenation time.

A different behavior of hydrogen has been observed in hydrogenated Mg films deposited on the stainless steel substrate (Fig. 2). The XRD pattern of the as-deposited Mg film also includes a single h-Mg (0 0 2) characteristic peak at 34.5° (Fig. 2, curve a) with a width corresponding to a mean crystallite size of ~95 nm. After 15 min of hydrogenation, the intensity of this h-Mg (0 0 2) peak decreases and the t-MgH_2 (1 1 0), (1 0 1) and (2 0 0) peaks appear at 28.0°, 35.8° and 40.3°, respectively (Fig. 2, curve b). After 30 min of hydrogenation, the h-Mg (0 0 2) peak from metallic Mg no longer appears on the XRD pattern indicating that Mg is completely transformed into MgH_2 (Fig. 2, curve c).

The volume fraction of MgH_2 hydride phase in Mg film was evaluated using the peak amplitudes [13]. Fig. 3 gathers the time evolution of this volume fraction for Mg films on quartz hydrogenated at 220 °C (curve 1) and 250 °C (curve 2) and Mg films on stainless steel hydrogenated at 220 °C (curve 3). It is seen that Mg film on the stainless steel substrate is completely converted into MgH_2 after 45 min (Fig. 3, curve 3). For Mg films on quartz, the transformation remains partial even after 20 h of hydrogenation at 250 °C (Fig. 3, curve 2).

The changes of film color have been registered when hydrogenation is performed in a transparent quartz tube. For Mg films deposited on the stainless steel substrate, the shiny metallic film

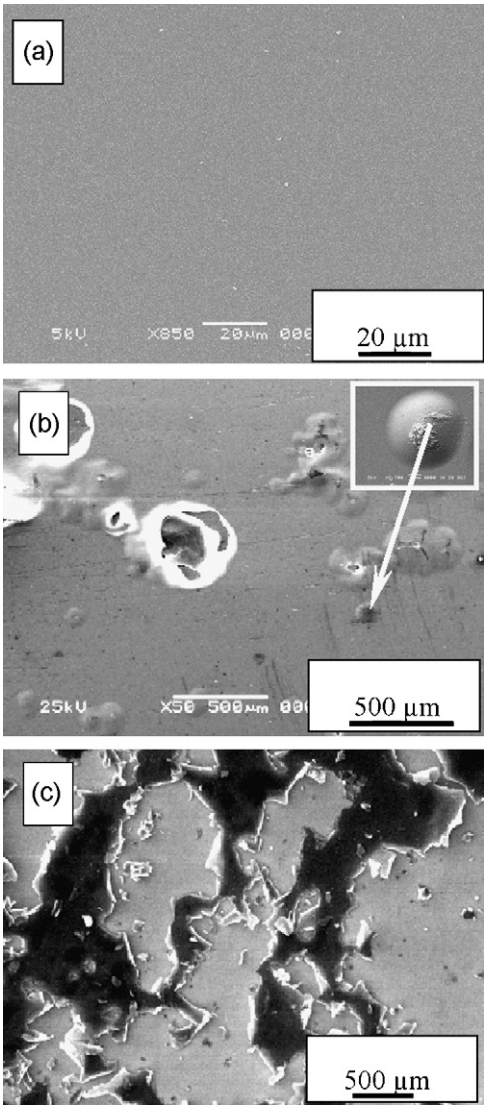

Fig. 4. SEM surface views of the Mg film on quartz for hydrogenation durations: (a) as-deposited, (b) 0.5 h, and (c) 6 h.

color changes into dark brown after 5 min of hydrogenation as sample temperature reaches 100 °C. After 10 min of hydrogenation and as the sample temperature reaches 150 °C, the film becomes transparent indicating that stoichiometric MgH_2 compound is formed. Upon further hydrogenation, a cracking process starts and the film is transformed into black powder. For films on the quartz substrate, the shiny metallic film color changes into opaque after 10 min of hydrogenation as sample temperature reaches 150 °C and remains unchanged upon ensuing hydrogenation. A noteworthy point is that reproducibility of these results is poor and it explains the observed experimental dissimilarities between different groups of researchers.

The changes of surface topography give complementary information about the stress relaxation processes induced by hydrogenation. The surface morphology was investigated by SEM in the as-deposited state and after different stages of hydrogenation. It is registered that hydrogenation and its associated stresses build-up affects the surface topography of the Mg film in different ways when it is deposited on quartz (Fig. 4) or on stainless steel (Fig. 5).

Images of the as-deposited Mg film, either on quartz (Fig. 4a) or stainless steel, are consistent with a columnar structure which includes many well defined boundaries which are open and may serve as channels for the transportation of hydrogen from the surface into the bulk. It is in agreement with earlier observations [4]. Under hydrogenation, the induced stress is sufficient to produce large (10–500 μm) disconnected buckles on the Mg film deposited on quartz (Fig. 4b). Buckles reach 0.5 μm in height for a lateral extension of 10–15 μm. These buckles indicate a reduction in the clamping to the substrate. Furthermore, this irreversible pattern evolves with hydrogenation time as the buckles start to branch and interconnect until the film is completely cracked and delaminated (Fig. 4c).

Rather different SEM surface views have been observed for hydrogenated Mg films deposited on the stainless steel substrate (Figs. 5): film cracking (Fig. 5a), fragmentation (Fig. 5b) and eventually apparent clustering of small-sized particles (Fig. 5c). The later observation is consistent with the decrepitation of the materials into nanometer-size powder [14]. It has been registered that as-deposited Mg films consist of grains with mean diameter of 80–90 nm whereas in the hydrogenated ones the size of grains decreases down to 25–30 nm.

Different hydrogenation behaviors of Mg films have been observed depending on their coupling with the substrate: (i) on

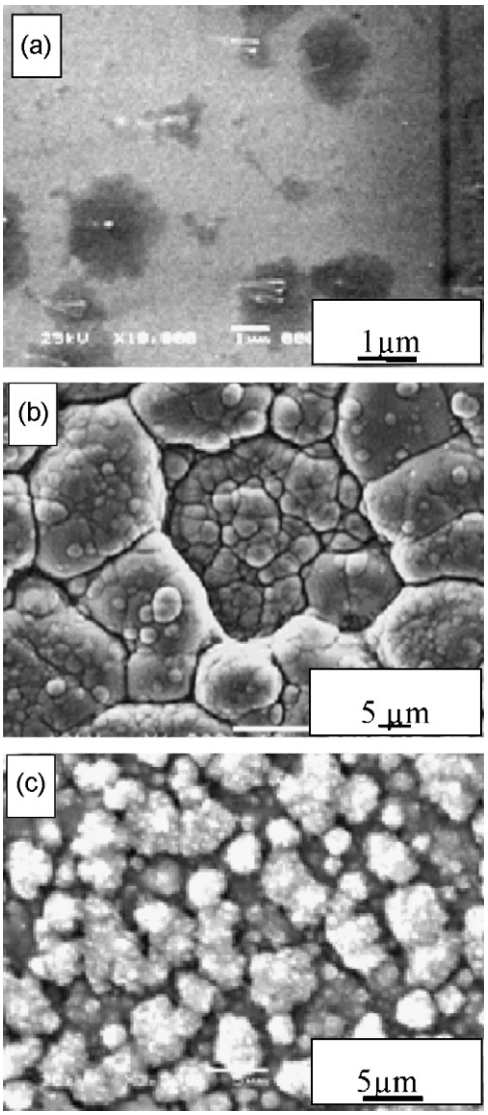

Fig. 5. SEM surface views of Mg films on stainless steel for hydrogenation durations: (a) 5 min, (b) 30 min, and (c) 60 min.

quartz, slow and partial hydrogenation of Mg film accompanied by formation of buckles and lifted flakes on the surface and (ii) on stainless steel, fast and complete hydrogenation of Mg film together with clusters of decrepitated nanometric MgH_2 crystallites.

These observations can be analyzed on the basis of recent understanding about the dynamic properties of adsorbate and the transport of adsorbed particles along grain boundaries of nanometer-size materials [15]. As rapid uptake of hydrogen through the grain boundaries in open contact with the hydrogen occurs, plastic deformation and grain fragmentation take place with lateral slow inward diffusion of hydrogen through the grain boundaries. The high compressive stresses lead to film detachment in a form of buckling when the film is weakly adhered to the substrate. The structure eventually fails by adhesive film debonding from the surface of the substrate.

The observations reveal that Mg film deposited on the quartz detached from the substrate before the complete transformation of Mg into MgH_2. Film is lifted by a mechanism involving buckle formation at the interface followed by buckle growth, subsequent coalescence and by the separation of the interface producing macroscopic flakes. The growth of the interfacial cracks and the subsequent evolution of these cracks into flake structure are strongly dependent on both the rheological properties of the film and the nature of the surface of the substrate [16]. Aspects of the failure sequence may change with the Mg layer thickness. Buckling is an effective mechanism to reduce stress locally; for example, the elastic energy stored in a clamped film is reduced by more than 90% in the buckled areas of films of comparable thickness [17].

A fast and complete transformation of Mg into MgH_2 is registered for Mg films deposited on the stainless steel substrate. These apparent discrepancies can be understood by considering the differences in the coupling occurring between the film and the substrate during hydrogenation. When the film has a strong adherence to the substrate, the observed buckle-and-crack network can be attributed to MgH_2 precipitation within the Mg film [18] and hydrogen-induced deformation processes. Mechanical property tests show that solute hydrogen reduces the yield strength of ductile specimens and decreases the fracture stress [19]. The atomic hydrogen interacts at the sites formed during film bulk cracking process and produces a hydride which, in turn, activates formation of new cracks. Therefore, spontaneous film cracking may be maintained by the hydrogenation process. According to the suggested scheme, the generation rate of new sites for hydrogen rather than the strain is the major factor for hydrogenation kinetics. This is in agreement with previous results [20,21] which recently confirmed that when the mechanical stress is removed, thermodynamic data mainly reflect the bulk. Similarly, investigation of ball-milled MgH_2 samples using inelastic neutron scattering revealed a stress-release upon hydrogenation.

4. Conclusions

The experimental results were analyzed in terms of correlations between the film and the substrate coupling processes and the very large deformations of the film under hydrogenation, which are responsible for the macroscopic mechanical response of the film. When the Mg film is weakly adhered to the substrate, the stresses induced by hydrogenation initiate film buckling with the creation of a buckle-and-crack network. Film is therefore detached in the form of flakes before complete transformation of Mg into MgH_2. If there is a strong coupling between the film and the substrate as for Mg on stainless steel, a fast and complete transformation of Mg into MgH_2 takes place, accompanied by cracking and fragmentation processes and eventually spontaneous crashing resulting into powder of stoichiometric hydride.

These results are in agreement with the assumption that the major factor for hydrogenation kinetics is the generation rate of new sites for hydrogen initiated by structural rearrangements upon hydrogenation. The present study contributes to the understanding of the influence of Mg film/substrate coupling on the hydride growth mechanism and leads to an improved assessment of the comparability of the experimental results about hydrogen behavior in thin film and bulk materials.

Acknowledgement

This work has been financially supported by Lithuanian Science Foundation Project: “Development of multifunctional material heterostructures for hydrogen fuel cells” (Contract No. C-15/2008/02, Acronym: H_2 technologijos).

References

[1] Y.P. He, Y.P. Zhao, J. Alloys Compd. 482 (2009) 173.
[2] M. Dornheim, S. Doppiu, G. Barkhordarian, U. Boesenberg, T. Klassen, O. Gutfleisch, R. Bormann, Scr. Mater. 56 (2007) 56.
[3] J.A. Thornton, D.W. Hoffman, J. Vac. Sci. Technol. 14 (1977) 164.
[4] E. Wirth, F. Munnik, L.L. Pranevicius, D. Milcius, J. Alloys Compd. 475 (2009) 917.
[5] Y.H. Yu, M.O. Lai, L. Lu, P. Yang, J. Alloys Compd. 449 (2008) 56.
[6] A. Steuwer, J.R. Santisteban, M. Preuss, M.J. Peel, T. Buslaps, M. Harada, Acta Mater. 57 (2009) 145.
[7] Y. Tsushio, H. Enoki, E. Akiba, J. Alloys Compd. 281 (1998) 301.
[8] A. Borgschulte, J.H. Rector, B. Dam, R. Griessen, A. Zuttel, J. Catal. 235 (2005) 353.
[9] L. Aballe, C. Rogero, K. Horn, Phys. Rev. B 65 (2002) 125319.
[10] J.E. Castle, Electron. J. Spectrosc. Relat. Phenom. 106 (2000) 65.
[11] J.C. Bowman, J.A. Krumhansi, J.R. Stock, Appl. Phys. 26 (2009) 1057.
[12] JCPDS Data Cards, International Center of Diffraction Data, Swarthmore, PA, 1988.
[13] S. Rashkov, M. Monev, L. Tomov, Surf. Technol. 16 (1982) 203.
[14] J. Huot, M.L. Tremblay, R. Schulz, J. Alloys Compd. 356 (2003) 603.
[15] B. Fultz, H.N. Frase, Hyperfine Interact. 130 (2000) 81.
[16] H. Hirakata, T. Kitamura, T. Kusano, Eng. Fract. Mech. 72 (2005) 1892.
[17] S. Wagner, A. Pundt, Appl. Phys. Lett. 92 (2008) 051914.
[18] L.Z. Ouyang, H. Wang, C.Y. Chung, J.H. Ahn, M. Zhu, J. Alloys Compd. 422 (2006) 422.
[19] D. Teter, Acta Mater. 49 (2009) 4313.
[20] H.G. Schimel, M.R. Johnson, G.J. Kearley, A.J. Ramirez-Cuesta, J. Huot, F.M. Mulder, J. Alloys Compd. 393 (2005) 1.
[21] R. Gremaud, M. Gonzalez-Silveira, Y. Pivak, S. de Man, M. Slaman, H. Schreuders, B. Dam, Acta Mater. 57 (2009) 1209.